GC response factors for products **6a**, **6c**, **7a**, and **7c** were determined with authentic samples; the GC response factor for **6b** was assumed to be equal to that of **6a**. The mean concentration of PhSeH was the average of the initial and final concentrations of PhSeH where the final concentration of PhSeH was calculated as the initial concentration of PhSeH minus the initial concentration of PTOC ester **5**.

Acknowledgment. We thank the National Science Foundation (CHE-9117929) for support and Dr. K. U. Ingold for a constructive discussion.

Ultrafast Studies of Photochromic Spiropyrans in Solution

Jin Z. Zhang,† Benjamin J. Schwartz, Jason C. King, and Charles B. Harris*

Contribution from the Department of Chemistry, University of California, Berkeley, California 94720, and Chemical Sciences Division, Lawrence Berkeley Laboratory, Berkeley, California 94720. *Received August 10, 1992*

Abstract: The photochromic reaction dynamics of the spiropyran molecule 1′,3′,3′-trimethyl-6-hydroxyspiro[2*H*-1-benzopyran-2,2′-indoline] (HBPS) in solution have been studied with picosecond and femtosecond transient electronic absorption spectroscopy. Following excitation near 300 nm, the C–O bond of the molecule breaks in less than 100 fs to form a metastable species. A small fraction of this metastable species re-forms the broken C–O bond on the time scale of 200 fs. The major fraction of the metastable photoproduct vibrationally relaxes in a few picoseconds, and then undergoes isomerization to form a merocyanine product with a decay time constant of about 100 ps, depending on solvent viscosity. This isomerization decay is faster at shorter probe wavelengths and slower at longer wavelengths, indicating that this isomerization gives rise to a red-shifted absorption spectrum. The final merocyanine isomers are stable on the nanosecond time scale. All the results indicate that the initial steps of the photochromic reaction process of HBPS are extremely fast.

Introduction

Photochromism, first discovered in 1876,[1] is a phenomenon in which a compound changes color when exposed to light of one wavelength and reverts to its original color when irradiated with light of a different wavelength. Studies on photochromic substances were quite limited before 1930,[2-6] but the period from 1940 to 1960 saw an increase of interest in these substances.[7-10] A number of review articles[11-13] have been published outlining the development of thought regarding photochromism, and several books[14-16] have been devoted specifically to this subject. A variety of organic as well as inorganic compounds were found to exhibit photochromism both in the solid state and in solutions.[7-16] Recently there has been a renaissance in the study of photochromic materials[15-29] due to their potential applications in several important areas, including high-density optical storage, optical switching, image processing, and displays.[7,15,27]

One of the most important classes of photochromic materials is spiropyran compounds. These compounds have been studied extensively,[19-30] with the nitro derivatives of spirobenzopyran receiving the most attention.[19-22] Several models have been proposed to explain the properties and photochromic reaction mechanisms of these molecules based on both frequency domain[7-18] and time domain[19-28] spectroscopic studies. Time-resolved experiments have been carried out using techniques such as laser flash photolysis[19-23] and time-resolved resonance Raman scattering.[24,25] These studies found that the reaction dynamics for spiropyrans with a nitro group are significantly different from those for spiropyrans without a nitro group. A triplet state was found to play an important role in the photochemical reaction process of spiropyrans containing a nitro group, as indicated by the sensitivity of the dynamics to the presence of O_2.[19-22] For molecules containing no nitro group, the photoreaction was dominated by singlet states. These studies have improved the understanding of the reaction mechanisms of photochromic spiropyrans.

Previous studies have also found that the photochromic reaction of spiropyran molecules features the dissociation of a C–O bond, producing a distribution of isomers.[19-30] However, the rate and mechanism of the initial reaction steps for these molecules are yet to be determined. Furthermore, there is still no consistent model to explain all of the experimental observations due to the extremely fast C–O dissociation rate and to the complications caused by the presence of more than one merocyanine isomer produced in the reaction process.[27]

The advent of femtosecond lasers has made it possible to study extremely fast rate processes directly. The experiments carried

† Present address: Department of Chemistry and Biochemistry, University of California, Santa Cruz, CA 95064.

(1) ter Meer, E. *Justus Liebigs Ann. Chem.* **1876**, *181*, 1.
(2) Marckwald, W. *Z. Phys. Chem. (Leipzig)* **1899**, *30*, 140.
(3) Wislicenus, W. *Justus Liebigs Ann. Chem.* **1893**, *277*, 366.
(4) Biltz, H.; Wienands, A. *Justus Liebigs Ann. Chem.* **1899**, *308*, 1.
(5) Harris, L.; Kaminsky, J.; Simard, R. G. *J. Am. Chem. Soc.* **1935**, *57*, 1151.
(6) Gheorghiu, C. V.; Matei, V. *Bull. Soc. Chim. Fr.* **1939**, *6*, 1324.
(7) Fischer, E.; Hirshberg, Y. *J. Chem. Soc.* **1952**, 4522.
(8) Hirshberg, Y.; Fischer, E. *J. Chem. Soc.* **1953**, 629; **1954**, 297, 3129.
(9) Heiligman-Rim, R.; Hirshberg, Y.; Fischer, E. *J. Chem. Soc.* **1961**, 156; **1962**, *66*, 2465, 2470.
(10) Hirshberg, Y. *J. Am. Chem. Soc.* **1956**, *78*, 2304.
(11) Brown, G. H.; Shaw, W. G. *Rev. Pure Appl. Chem.* **1961**, *11*, 2.
(12) Day, J. H. *Chem. Rev.* **1963**, *63*, 65.
(13) Exelby, R.; Grinter, R. *Chem. Rev.* **1965**, *65*, 247.
(14) Brown, G. H., Ed. *Photochromism*; Wiley: New York, 1971.
(15) El'tsov, A. V. *Organic Photochromes*; Consultants Bureau: New York, 1990.
(16) Dürr, H., Bouas-Laurent, H., Eds. *Photochromism: Molecules and Systems*: Studies in Organic Chemistry 40; Elsevier: Amsterdam, 1990.
(17) Kurita, S.; Kashiwagi, A.; Kurita, Y.; Miyasaka, H.; Mataga, N. *Chem. Phys. Lett.* **1990**, *171*, 553.
(18) Heller, H. G. *Chem. Ind.* **1978**, *18*, 193.
(19) Krysanov, S. A.; Alfimov, M. V. *Laser Chem.* **1984**, *4*, 129.
(20) Krysanov, S. A.; Alfimov, M. V. *Chem. Phys. Lett.* **1982**, *91*, 77.
(21) Kallsky, Y.; Orlowski, T. E.; Williams, D. J. *J. Phys. Chem.* **1983**, *87*, 5333.
(22) Lenoble, C.; Becker, R. S. *J. Phys. Chem.* **1986**, *90*, 62.
(23) Lenoble, C.; Becker, R. S. *J. Photochem.* **1986**, *34*, 83.
(24) Aramaki, S.; Atkinson, G. H. *Chem. Phys. Lett.* **1990**, *170*, 181.
(25) Aramaki, S.; Atkinson, G. H. *J. Am. Chem. Soc.* **1992**, *114*, 438.
(26) Ernsting, N. P.; Dick, B.; Arthen-Engeland, Th. *Pure Appl. Chem.* **1990**, *62*, 1483.
(27) Ernsting, N. P.; Dick, B.; Arthen-Engeland, Th. *J. Phys. Chem.* **1991**, *95*, 5502.
(28) Tamai, N.; Masuhara, H. *Chem. Phys. Lett.* **1992**, *191*, 189.
(29) Yoshida, T.; Morinaka, A.; Funakoshi, N. *J. Chem. Soc., Chem. Commun.* **1988**, 437.
(30) Bertelson, R. C. In *Photochromism*; Brown, G. H., Ed.; Wiley: New York, 1971; p 45.

0002-7863/92/1514-10921$03.00/0

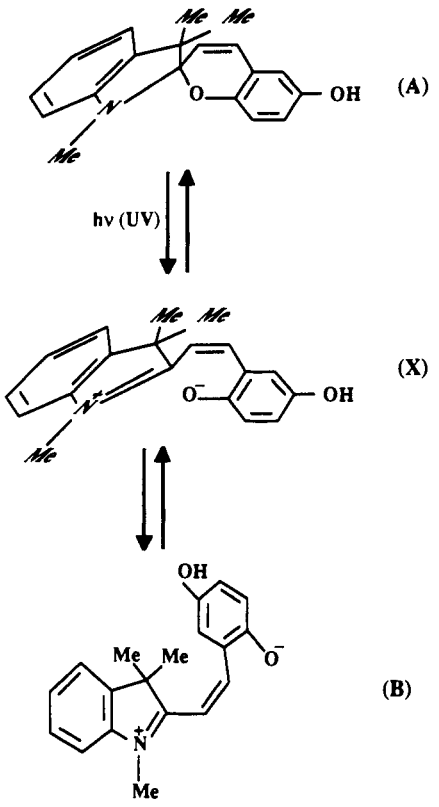

Figure 1. Structure and proposed reaction process of HBPS. A is the parent molecule HBPS in its ground electronic state, X denotes the nascent photoproduct, and B represents one of the several possible merocyanine isomers.

out by Ernsting and Arthen-Engeland were the first directed toward the study of the ultrafast photochromic reaction dynamics.[26,27] They studied indolinespiropyrans in *n*-pentane and found that the first merocyanine isomer is formed in its ground electronic state in 0.9–1.4 ps. They further reported that the internally hot (~900 K) primary merocyanine product may isomerize on the picosecond time scale, resulting in a distribution of isomers. Very recently, Tamai and Masuhara reported an investigation of the photochromic reaction of a spirooxazine with 200-fs time resolution.[28] The rate constants for the C–O bond cleavage and relaxation from a "transition state" to a metastable merocyanine were estimated to be approximately 700 and 470 fs^{-1}, respectively. Tamai and Masuhara suggested that thermal relaxation could play an important role in the merocyanine dynamics. Both of the above studies indicate that the C–O bond dissociation is indirect; that is, it takes several vibrational periods to cleave the C–O bond. This is in contradiction with other observations which suggest that the C–O dissociation is direct.[27,31] Thus, the rate for C–O dissociation and the time scale for product isomerization need further investigation.

1′,3′,3′-trimethyl-6-hydroxyspiro[2*H*-1-benzopyran-2,2′-indoline] (HBPS), shown in Figure 1A, is a very interesting molecule because in solid films this compound has the unique property of being photochromic between two different colored states produced by photoexcitation of the colorless parent molecule.[29] This is different from most of the other photochromic spiropyrans, in which photochromism occurs between the parent molecule and one of its merocyanine photoproducts. Thus far, no study has been conducted on HBPS in solutions. In this paper we report the first experimental investigation of the photochromic reaction dynamics of HBPS in solutions, with a focus on the time scale from 100 fs to a few nanoseconds. The C–O dissociation rate and the formation rate of the first merocyanine isomer were measured directly. The subsequent energy relaxation dynamics of the nascent photoproduct and the redistribution of the isomers

(31) Bagchi, B.; Fleming, G. R. *J. Phys. Chem.* **1990**, *94*, 9.

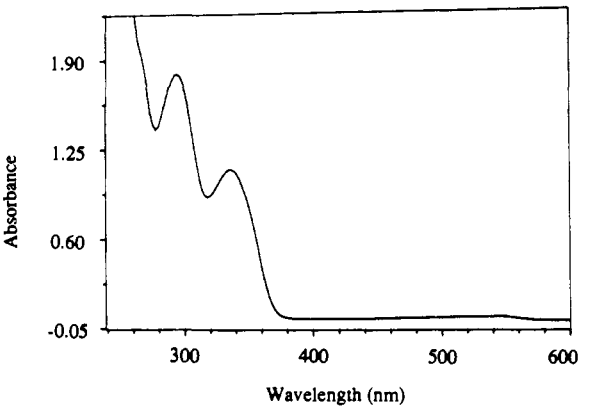

Figure 2. Electronic absorption spectrum of 0.1 mM HBPS in 1-propanol at room temperature.

were monitored up to 4 ns. The effects of temperature, solvent polarity, and viscosity on the dynamics were also investigated. A simple model is proposed to explain the observed data. In the next section, the experimental apparatus and procedure are outlined, followed by a presentation of the results obtained and a discussion of possible models to interpret the data.

Experimental Section

The experiments were performed with either a femtosecond or a picosecond laser system. Both laser systems have been described before.[32,33] Briefly, the picosecond laser pulses were generated by a dye laser (Coherent, CR-599) synchronously pumped by an Ar^+ laser (Spectra-Physics, Model 2030) and amplified at 10 Hz in a three-stage dye amplifier pumped by a Q-switched Nd:YAG laser (Molectron 34-10).[32] The final output (1 mJ/pulse, 590 nm, and 1 ps fwhm) was frequency-doubled in a KDP crystal to produce about 100 μJ of 295-nm UV light. This UV pulse was time-delayed with respect to the residual 590-nm light with a translation stage and then used to excite the molecules. The residual 590-nm light was focused into a water cell to generate a white light continuum. The photoproducts generated by photolysis of the parent molecules were probed at the desired wavelength selected from the white light continuum through band-pass filters (10 nm fwhm). The experiments were performed by splitting the probe beam into signal and reference beams which were detected by two silicon photodiodes (EG&G Electro-Optics, DT-110). A 2 mM sample solution was prepared by dissolving HBPS (Eastman Kodak) in 1-propanol (Fisher Chemical, spectrograde). To avoid photoproduct buildup, either a 1-mm quartz flow cell or a 100-μm flow jet was used. The UV light was focused collinearly with the signal beam into the sample with a 10-cm-focal-length lens. Signals from the solvent molecular ions due to multiphoton ionization were observed when high UV intensity was used; thus, the UV power was attenuated to a point (around 3 μJ) such that no signal was observable from the corresponding pure solvent.[34]

For the femtosecond laser system,[33] a cavity-dumped CPM laser was amplified by a copper vapor laser-pumped, 6-pass bow-tie amplifier to produce 620-nm, 100-fs pulses (3 μJ/pulse) at 8 kHz. This output was doubled in a 300-μm KDP crystal to produce 0.5-μJ, 310-nm pulses. The UV light was used to excite the sample, and the residual fundamental light was spatially filtered and used to probe the resulting dynamics. The delay stage, data acquisition, and analysis were similar to those of the picosecond system described above. The pump and probe beams were focused through the sample (a 100-μm flow jet) with a 10-cm-focal-length lens at a 10° angle, giving an estimated spot size of 50 μm. As with the above experiment, care was taken to assure that the signal was linear with respect to pump power and that there was no signal from the blank solvent. A flow jet for the sample was necessary in this case to ensure that the photoproducts with long lifetimes generated from one laser pulse did not interfere with the dynamics in the next laser pulse.

Results

The electronic absorption spectrum of HBPS in 1-propanol at room temperature is shown in Figure 2. In the near-UV region there are two strong broad bands peaked around 300 and 345 nm, respectively, which are very similar to those observed in the

(32) Harris, A. L.; Berg, M.; Harris, C. B. *J. Chem. Phys.* **1986**, *84*, 788.
(33) Schwartz, B. J.; Peteanu, L. A.; Harris, C. B. *J. Phys. Chem.* **1992**, *96*, 3591.
(34) Zhang, J. Z.; Harris, C. B. *J. Chem. Phys.* **1991**, *95*, 4024.

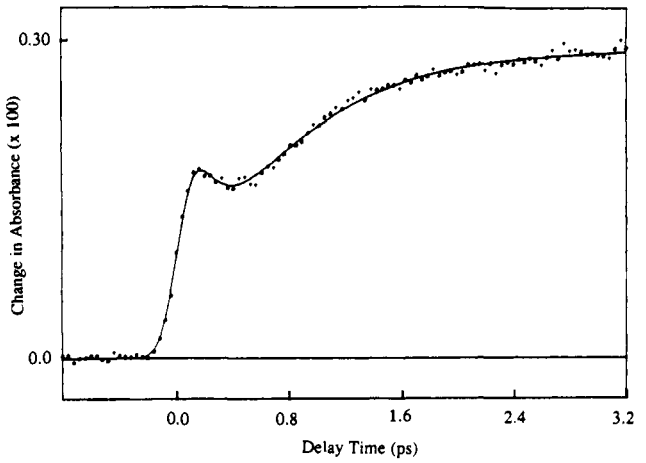

Figure 3. Transient absorption spectrum of 2.0 mM HBPS in 1-propanol excited with 310-nm light and probed at 620 nm. The circles are experimental data, and the solid curve is a fit to an exponential decay (180 fs) and an exponential rise (>700 fs) plus an offset.

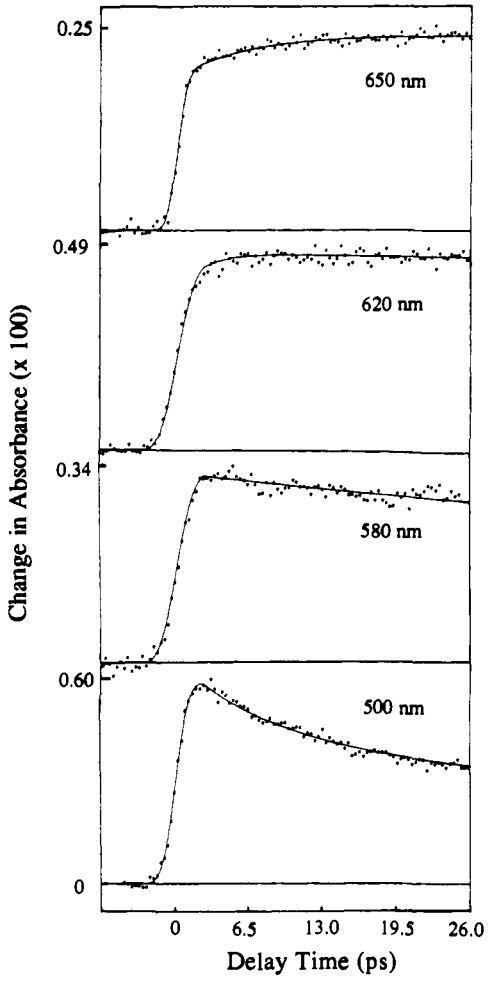

Figure 4. Transient absorption spectrum of 2.0 mM HBPS in 1-propanol pumped with 295-nm light and probed at a variety of wavelengths on the time scale from 1 to 25 ps.

spectrum for solid HBPS in a thin film.[29] The 1-propanol solution of HBPS exhibits a slightly red color, as is evident from an extremely weak band around 550 nm in the absorption spectrum. This red color is probably caused by the presence of a small amount of residual merocyanines in the sample. The current investigation is focused on the intense 300-nm band; the very weak visible absorption is not expected to interfere with the experiment. The solid-film study demonstrated that the transient absorption spectrum of the photoproduct from UV photolysis has two bands

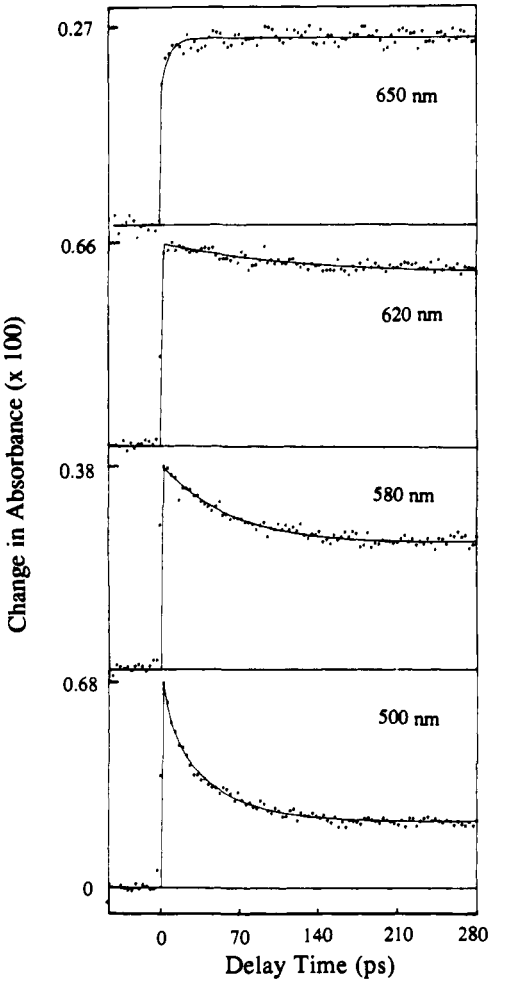

Figure 5. Transient absorption spectrum of 2.0 mM HBPS in 1-propanol pumped with 295-nm light and probed at a variety of wavelengths on the time scale from 1 to 280 ps.

peaked around 400 nm (blue) and 600 nm (red).[29] In the present study, the dynamics of the photoproducts in solution are monitored by varying the probe wavelength across these two bands.

Figure 3 shows the transient spectrum of HBPS in 1-propanol when the solution is excited at 310 nm and probed at 620 nm with 100-fs laser pulses. The spectrum features a pulse-width-limited rise with a fast decay, followed by a "slow" rise. The data are fit with a single exponential decay with a time constant of 180 fs and a single exponential rise of ≤2 ps plus an offset, convoluted with a Gaussian of 100 fs to represent the laser pulse. The pulse-width-limited rise (<100 fs) indicates that the newly formed species is generated in <100 fs. The subsequent fast decay shows a disappearance of the species on the time scale of 180 fs. Apparently, the "slow", ≤2-ps rise is an indication of population growth of this species or an increase in absorbance due to another species (e.g., an isomer) absorbing at 620 nm.

The dynamics on longer time scales were followed by using a picosecond laser system with 295-nm pump pulses and a variety of probe wavelengths. The same electronic state is reached with the 295-nm light and the 310-nm light; thus the subsequent reaction dynamics are expected to be the same, or at least very similar. Figure 4 shows the transient spectrum from 1 to 26 ps for several different probe wavelengths (500–650 nm), covering the red transient absorption band.[29] Figures 5 and 6 show scans for the same probe wavelengths on much longer time scales (up to about 1 ns). Scans with various time scales are necessary for appropriate data fitting as well as for better visualization of the dynamics. For each probe wavelength, the transient decay spectra typically feature a pulse-width-limited rise (<1 ps) and then a rise or decay (depending on the probe wavelength) with a time constant of a few picoseconds, followed by a slower decay on a

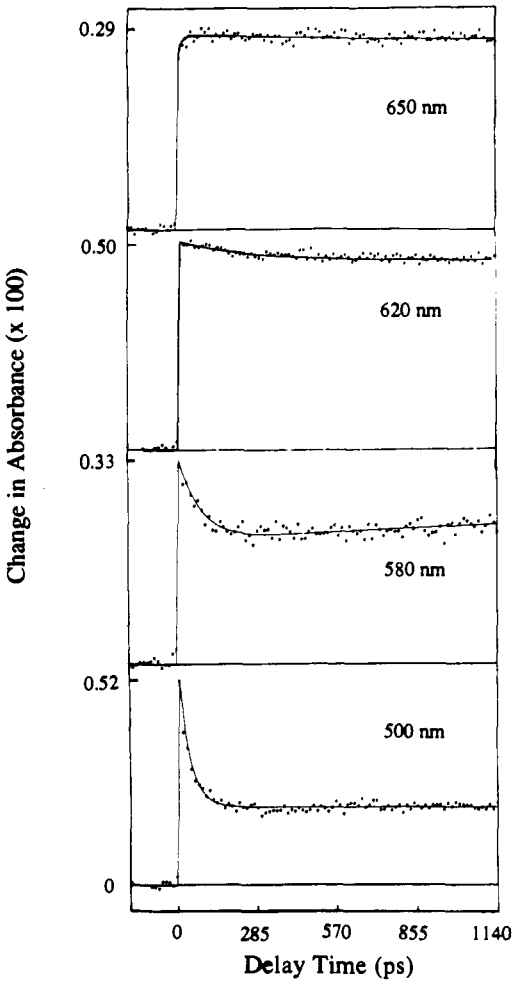

Figure 6. Transient absorption spectrum of 2.0 mM HBPS in 1-propanol pumped with 295-nm light and probed at a variety of wavelengths on the time scale from 1 ps to 1.2 ns.

45–180-ps time scale. The spectrum does not change on nanosecond time scales, as confirmed by additional scans out to 4 ns.

To obtain a more quantitative understanding of the dynamics, the experimental data were fit with a simple analytical function. The fit (solid curve) to the data (dots) for each probe wavelength was performed by using either a double-exponential decay with an offset (500 and 580 nm) or a single-exponential rise plus a single-exponential decay with an offset (620 and 650 nm), convoluted with a Gaussian of about 1 ps. Several features observed in these transient spectra are worth discussion. At 620 nm, the pulse-width-limited rise is consistent with the femtosecond data discussed above, where a 100-fs pulse-width-limited rise was observed. Then, the fast rise (≤2 ps) (Figure 4) corresponds to the "slow" rise observed in the femtosecond data (Figure 3). The long time decay feature has a time constant of around 180 ps (Figures 5 and 6). A closer examination of Figures 5 and 6 reveals a sensitive dependence of the dynamics on the probe wavelength. For instance, the 180-ps decay component observed at 620 nm becomes much faster at 580 nm (64 ps) and 500 nm (45 ps) but disappears at 650 nm. Thus, the general trend is that the decay becomes faster at shorter wavelengths, suggesting a red shift of the transient absorption spectrum of the photoproduct. Furthermore, the fast, ≤2-ps rise observed at 620 nm becomes slower at 650 nm (6 ps). At bluer wavelengths, such as 580 nm, this fast component disappears; at even bluer wavelengths, such as 500 nm, instead of showing a fast rise, the spectrum displays a fast 6-ps decay. The parameters used in fitting the data are summarized in Table I.

In addition to the red transient absorption band at 500–700 nm, the blue transient absorption band that is peaked around 400 nm was also examined. When probed at 450 nm, the transient

Table I. Fitting Parameters for Different Probe Wavelengths and Solvents[a]

solvent	wavelength (nm)	time constant (ps)	preexponential factor[b]
1-propanol	450	8 ± 2	0.40
		106 ± 5	0.20
		offset	0.43
	500	6 ± 2	0.15
		45 ± 5	0.31
		offset	0.22
	580	64 ± 5	0.14
		offset	0.24
	620	2 ± 1	−0.05
		180 ± 5	0.11
		offset	0.55
	650	6 ± 2	−0.05
		offset	0.25
methanol	580	36 ± 5	0.14
		offset	0.31
1-hexanol	580	101 ± 5	0.18
		offset	0.41
cyclohexane	580	40 ± 5	0.15
		offset	0.32

[a] The fits to the data are performed using either a double-exponential decay with an offset or a single-exponential rise plus a single-exponential decay with an offset, convoluted with a Gaussian of about 1 ps. [b] Positive to indicate a decay and negative to indicate a rise.

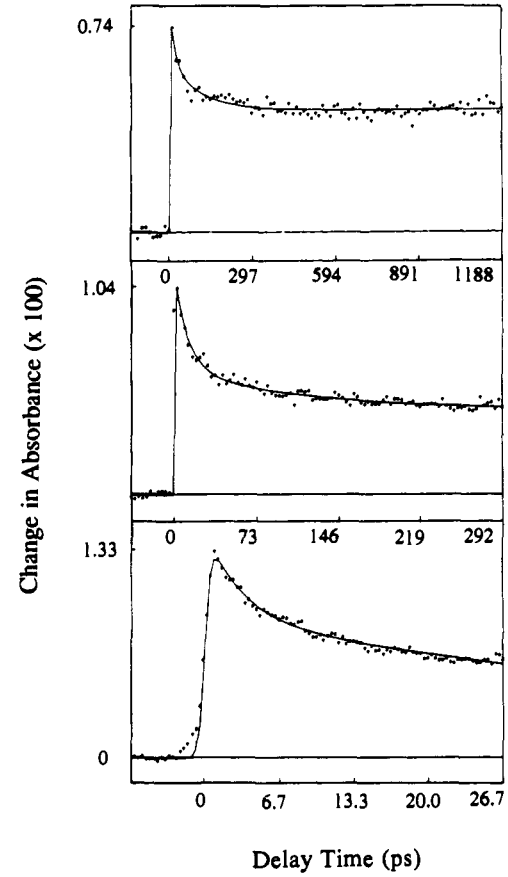

Figure 7. Transient absorption spectrum of 2.0 mM HBPS in 1-propanol pumped with 295-nm light and probed at 450 nm for different delay-time ranges.

spectra for different time scans (Figure 7) showed qualitatively similar features to those observed for the 600-nm band (Figures 4–6). This suggests that the same species is responsible for both the 400 and 600 nm bands and that these bands correspond to two different electronic transitions of this species. This interpretation is consistent with the solid-film study[29] and studies on similar spiropyrans.[19-28] Quantitatively, the decay time constants are different from those of the 600-nm band. For example, the fast and slow decays are 8 and 106 ps, respectively, suggesting

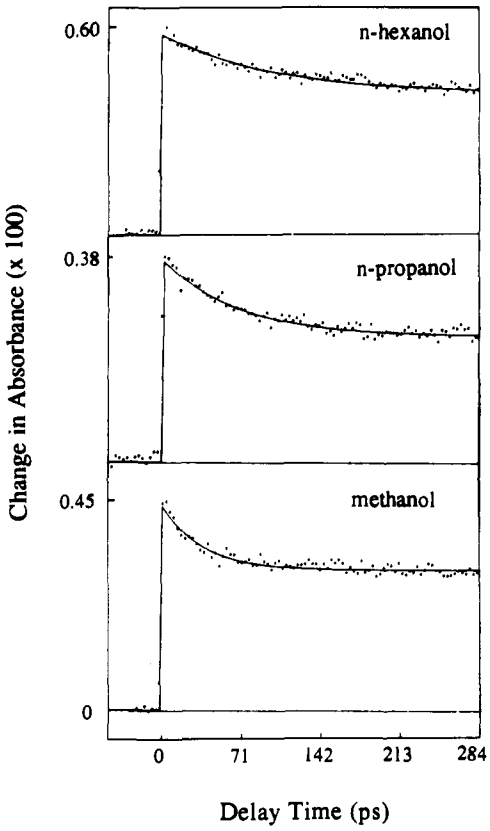

Figure 8. Transient absorption spectrum of HBPS pumped with 295-nm light and probed at 580 nm for different solvents.

that the spectrum shift rate is different for the 400-nm band compared to the 600-nm band.

Preliminary experiments were also carried out to examine the dependence of the dynamical features on parameters such as the solution temperature, solvent viscosity, and solvent polarity. The effect of temperature on the dynamics was studied by performing the experiments in 1-propanol at 0 and −78 °C. Lowering the temperature is expected to slow down processes such as diffusion-controlled C–O bond re-formation or merocyanine isomerization. The data obtained at these temperatures failed to reveal any significant change in the dynamics compared to those observed at room temperature. It should be interesting to conduct the experiment at even lower temperatures. However, this is currently limited by the experimental apparatus available.

Investigation of the solvent dependence of the dynamics shows that the observed dynamical features, especially the slow-decay component, are sensitive to the viscosity of the solvent. Measurement of the transient spectra in several alcohols with very different viscosities at the same probe wavelength (580 nm) shows a drastic change in the decay rate. The time constants are 36 ps for methanol (viscosity 0.6 cP), 64 ps for 1-propanol (2.2 cP), and 101 ps for 1-hexanol (5.4 cP). This demonstrates a clear correlation between the decay time and the viscosity of the solvent: slower decays for larger viscosities. The decay time is roughly proportional to the viscosity, consistent with diffusive models. This slow-decay component was also measured in a nonpolar solvent, cyclohexane, and it was found that the decay time at 580 nm (40 ps) is essentially the same as that in a polar solvent, methanol (36 ps). The viscosities of cyclohexane and methanol are very similar, 0.66 and 0.60 cP, respectively. Thus, this result indicates that the slow-decay dynamics are not particularly sensitive to solvent polarity or polarizability. A more detailed discussion of the experimental results and possible interpretations of the data are given next.

Discussion

Molecular Structure and Electronic Absorption Spectrum. The HBPS molecule consists of a 2*H*-pyran moiety and a second moiety that are orthogonal to each other and are held together by a common spiro carbon atom (Figure 1A). The interaction between the π-electron systems of these two parts is not significant, as the moieties are not coplanar and there is no conjugation between them; thus, the absorption spectrum of the molecule resembles the sum of the spectra for the two parts.[35] The molecule therefore does not absorb in the visible region and appears colorless. As mentioned above, excitation of a solid HBPS film with UV light produces a species with two absorption bands in the visible peaked around 400 and 600 nm.[29] This is probably due to absorption by a planar merocyanine product having a conjugated π-electron system between the two parts of the molecule (Figure 1B). On the basis of studies performed on several similar spiropyran molecules in solids as well as in solutions,[19-30] the first step of the photoreaction is expected to proceed through the breaking of the C–O bond, resulting in the generation of a metastable species, labeled X in Figure 1. This nascent product is not stable since the two halves of the molecule are still orthogonal to each other. The molecule will subsequently rearrange (isomerize) to form a merocyanine species, labeled B, with the two parts of the molecule in the same plane. The π-electrons will conjugate, providing extra stability and causing the molecule to absorb in the visible. Several isomers are possible, and only one of them, B, is shown as an illustration. The following discussion is centered around the dynamics of the metastable species X and the isomers B.

Dynamics on the Femtosecond Time Scale: Direct Dissociation and Bond Re-Formation. The pulse-width-limited rise observed in the femtosecond data (Figure 3) shows that the species produced from 310-nm excitation of HBPS is generated in less than 100 fs. The initial rise is due to absorption by either the excited parent molecule, A*, or the newly formed species X. If the absorption is due to A*, an explanation for the subsequent 180-fs decay could be A* leaving the Franck–Condon region in the excited state, i.e., dissociation. If this was true, the 180-fs time constant would indicate indirect dissociation of the C–O bond. On the other hand, if the initial absorption is due to the nascent metastable species X, the fast rise would indicate that the dissociation of C–O occurs in less than 100 fs (essentially direct) and the 180-fs decay could be attributed to C–O bond re-formation, i.e., the X to A back-reaction. This process is equivalent to geminate recombination, where the initial pair of photofragments recombine following dissociation due to the "caging effect" of the solvent.[36,37] Without further information, it is difficult to decide which interpretation, indirect dissociation or direct dissociation/geminate recombination, better applies to the data.

Additional information about the dissociation comes from studies on similar spiropyrans and from comparison to other molecules. The direct dissociation model is consistent with a study carried out on spirooxazines and spironaphthopyrans by Aramaki and Atkinson.[24,25] Using transient absorption and transient resonance Raman techniques, they obtained data that also lead to the suggestion that C–O dissociation is direct. Direct dissociation is further supported by the fact that the quantum yield for the photochromic reaction of indolinespiropyrans does not depend on temperature in the range 0–100 °C,[41] and the fact that the reaction still proceeds at 4 K in a polymer matrix,[42] both of which point toward a photochemical reaction without an activation barrier.[27,31] It is also interesting to notice that the dynamical features observed for HBPS for the first few hundred femtoseconds

(35) Tyer, N. W., Jr.; Becker, R. S. *J. Am. Chem. Soc.* **1970**, *92*, 1289.
(36) Hynes, J. T. *Annu. Rev. Phys. Chem.* **1985**, *36*, 573.
(37) Harris, A. L.; Brown, J. K.; Harris, C. B. *Annu. Rev. Phys. Chem.* **1988**, *39*, 341.
(38) Joly, A. G.; Nelson, K. A. *Chem. Phys.* **1991**, *152*, 69.
(39) Harris, C. B.; King, J. C.; Schultz, K. E.; Schwartz, B. J.; Zhang, J. Z. *Ultrafast Phenom. 8*, in press.
(40) Schwartz, B. J.; King, J. C.; Zhang, J. Z.; Harris, C. B. *J. Chem. Phys.*, communication submitted.
(41) Dvornikov, A. S.; Malkin, Ya. N.; Kuz'min, V. A. *Izv. Akad. Nauk SSSR, Ser. Khim.* **1982**, *7*, 1520.
(42) Horie, K.; Hirao, K.; Kenmochi, N.; Mita, I. *Makromol. Chem., Rapid Commun.* **1988**, *9*, 267.

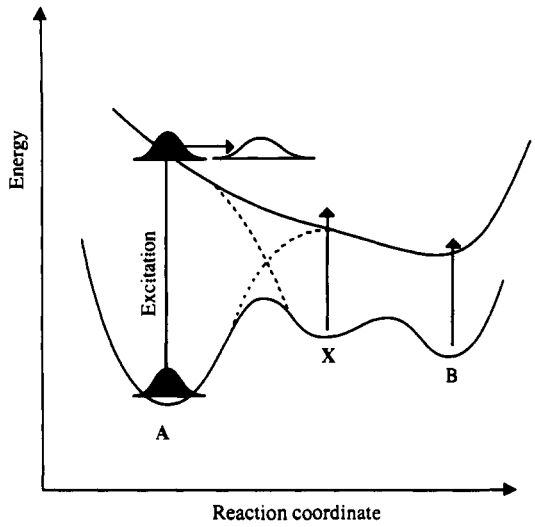

Figure 9. Schematic illustration of the photochemical reaction process of HBPS in a wave packet picture. X refers to the initial metastable product right after the C–O bond is broken. The solid curves represent the adiabatic surfaces, while the dashed lines indicate the diabatic surfaces. The reaction is proposed to proceed mainly along the diabatic surface, i.e., direct dissociation of the C–O bond. B represents one of the several possible merocyanine isomers. The reaction coordinate is somewhat arbitrary, but it represents the coordinate along which the wave packet motion dominates, e.g., a "normal mode coordinate" having characters of both C–O stretching and bending or rotation along a C–C bond of the molecule. These curves reflect the model in which the isomer B is more stable than X and its absorption spectrum is red-shifted with respect to that of X; both X and B are less stable compared to A in its ground electronic state.

are very similar to those seen for several molecules, including metal carbonyls in similar solvents.[38] Both explanations, indirect dissociation and geminate recombination, have been applied to interpret the similar fast rise and decay features observed in these systems.[38,39] However, a recent study of the directly dissociative molecule CH_2I_2 also shows similar dynamical features, strongly supporting the direct dissociation/geminate recombination model.[40] In the particular case of HBPS, the C–O re-formation is equivalent to the geminate recombination process in CH_2I_2 and metal carbonyls, but with a slightly faster rate due to the fact that the HBPS molecule never falls apart completely. As illustrated in Figure 9, the dissociation proceeds mainly along the purely repulsive, diabatic curve (dashed line) to produce X in its ground electronic state. Re-formation of the broken C–O bond in X is responsible for the 180-fs fast decay.

Dynamics on the Picosecond Time Scale: Vibrational Relaxation and Isomerization. The ≤2-ps rise observed at 620 nm and the 6-ps decay at 500 nm can be attributed to vibrational energy relaxation of the newly formed photoproduct, X, on the basis of a comparison with other, similar molecules which show vibrational relaxation on these same time scales.[43,44] The dominant feature on the picosecond time scale is the 45–180-ps decay, which is faster at shorter wavelengths and slower at larger wavelengths (Figures 4–7). This faster decay at shorter probe wavelengths (red-shifting spectrum) is in contrast to the typically observed blue shift for vibrational relaxation in many molecules in similar solvents.[34,43-49] Even though the reversed trend does not completely rule out the possibility of vibrational relaxation (depending on the Franck–Condon factors), it is very likely that a different mechanism is in operation in this case. An alternative explanation is that this red shift is due to isomerization. The existence of several merocyanine isomers has been suggested from previous experiments.[27] Figure 9 illustrates schematically this idea of a red-shifting spectrum when X isomerizes to form B, which absorbs at longer wavelengths. This interpretation is supported by a study of the viscosity dependence of the decay time constant, as will be discussed in more detail below.

The dynamics were monitored out to 4 ns, and the transient spectra do not show appreciable changes after a few hundred picoseconds. This shows that the merocyanine photoproducts live for many nanoseconds in room temperature solution after their formation. They could correspond to the colored states observed in solid HBPS films.[29] Direct confirmation of this would require performing the experiment out to a much longer time scale and, ideally, in low-temperature solutions.

Effect of Solvent Viscosity and Polarity. The dependence of the slow-decay component on the viscosity of the solvent was very clear from the data obtained in alcohols: slower decays for larger viscosities (Figure 8). This strongly supports the interpretation of isomerization. It is especially interesting to notice that the decay time constant appears to be linearly proportional to viscosity, which follows the Smoluchowski equation for diffusive isomerization.[50] An alternative explanation for this slow decay is solvation of the charge-separated photoproduct (dielectric relaxation) in the polar solvent.[51] This was tested by examining the dynamics in polar versus nonpolar solvents. At the same excitation wavelength (295 nm) and probe wavelength (580 nm), the decay is essentially the same in the nonpolar solvent cyclohexane (40 ps) as that in the polar solvent methanol (36 ps), two solvents with similar viscosities. This test strongly supports the explanation of isomerization over that of dielectric solvation since dielectric relaxation is expected to be sensitive to solvent polarity. Another possible explanation for the slow decay is secondary geminate recombination of the tethered C–O bond, similar to that observed by Scott and Doubleday in their study of azo compounds in liquid alkanes.[52] This explanation is not likely to hold for the case of HBPS; the transient spectra show a red shift, whereas secondary recombination would lead to a uniform decrease of the transient absorption band. In addition, the decay time scales are much shorter than those observed for tethered secondary recombination.[52] Thus, the slow (45–180 ps) decay can be reasonably assigned to isomerization.

Model for Photochromic Reaction. On the basis of this study and the discussion given above, a simple mechanistic model is proposed for the photoreaction of HBPS in room temperature solutions (see Figure 9). Excitation of the parent HBPS in its ground electronic state (A) near 300 nm promotes the molecule to one of its singlet excited states (A*). The molecule dissociates directly along the C–O bond in less than 100 fs, producing a metastable species (X). After its formation, this metastable species can revert to the parent molecule A in about 180 fs by undergoing geminate recombination on the ground-state PES, or it can vibrationally relax in a few picoseconds. This vibrational cooling is then followed by isomerization to form a more stable merocyanine product, B, on the time scale of ≥100 ps. The merocyanine species B absorbs at longer wavelengths compared to X, and more than one B isomer may be present in the solution. The various isomers are stable on the time scale of many nanoseconds. The two different photochromic states (II and III) discussed in ref 29 most likely correspond to the different merocyanine isomers.

Conclusions

In summary, the photochromic reaction dynamics of 1′,3′,3′-trimethyl-6-hydroxyspiro[2*H*-1-benzopyran-2,2′-indoline] in solutions have been studied with picosecond and femtosecond transient electronic absorption spectroscopy. The initial C–O bond dissociation is found to occur in less than 100 fs following UV

(43) Oxtoby, D. W. *Annu. Rev. Phys. Chem.* **1981**, *32*, 77.
(44) Chesnoy, J.; Gale, G. M. *Ann. Phys. (Paris)* **1984**, *9*, 893.
(45) Anfinrud, P. H.; Han, C. H.; Lian, T.; Hochstrasser, R. M. *J. Phys. Chem.* **1991**, *95*, 574.
(46) Xie, X.; Simon, J. D. *J. Am. Chem. Soc.* **1990**, *112*, 1130.
(47) Lee, M.; Harris, C. B. *J. Am. Chem. Soc.* **1989**, *111*, 8963.
(48) Wang, L.; Zhu, X.; Spears, K. G. *J. Phys. Chem.* **1989**, *93*, 2.
(49) Yu, S. C.; Xu, X.; Lingle, R., Jr.; Hopkins, J. *J. Am. Chem. Soc.* **1990**, *112*, 3668.
(50) McLennan, J. A. *Introduction to Non-equilibrium Statistical Mechanics*; Prentice-Hall Inc.: London; p 48.
(51) Castner, E. W., Jr.; Bagchi, B.; Maroncelli, M.; Webb, S. P.; Ruggiero, A. J.; Fleming, G. R. *Ber. Bunsen-Ges. Phys. Chem.* **1988**, *92*, 363.
(52) Scott, T. W.; Doubleday, C., Jr. *Chem. Phys. Lett.* **1991**, *178*, 9.

excitation. A small fraction of the dissociated molecules re-form the C–O bond on the time scale of 200 fs. The nascent photoproduct is found to vibrationally relax in a few picoseconds and to isomerize on the time scale of ≥100 ps. Further experiments need to be conducted to achieve a more complete understanding of the reaction mechanism, especially the dependence of the dynamics on solvent molecular structure and temperature.

Acknowledgment. This work was supported by the National Science Foundation. We also wish to acknowledge the U.S. Department of Energy, Office of Basic Energy Sciences, Chemical Sciences Division, under Contract No. DE-AC03-76SF00098, for some specialized equipment used in these experiments. B.J.S. gratefully acknowledges the support of graduate fellowships from the NSF and the W. R. Grace and Co. Foundation.

Submicron-Range Attraction between Hydrophobic Surfaces of Monolayer-Modified Mica in Water

Kazue Kurihara[‡] and Toyoki Kunitake*[,†]

Contribution from the Molecular Architecture Project, JRDC, Kurume Research Park, Kurume 830. Japan. *Received February 25, 1992. Revised Manuscript Received July 1, 1992*

Abstract: Very-long-range attraction extending to a separation close to 300 nm was observed between uncharged mica surfaces that are modified by hydrophobic layers of a polymerized ammonium amphiphile. The force distance profile in pure water is expressed by an exponential function composed of intensity parameter and decay length. Their values determined from the deflection method are 1.7 ± 0.5 mN/m and 62 ± 4 nm, respectively. The same parameters obtained from the jump-in method, 0.59 mN/m and 72 nm, agree within the experimental error. This hydrophobic layer is prepared by the Langmuir–Blodgett (LB) deposition in the *down-stroke* mode (transfer ratio: 0.8) and is stable enough to allow us to study salt effects on the attraction, practically for the first time. The intensity parameter decreases to 0.25 mN/m (from deflection) and 0.18 mN/m (from jump-in) with increasing NaBr concentrations to 10 mM, whereas the decay length remained unchanged at around 60 nm. Interestingly, hydrophobic surfaces prepared by monolayer transfer in the *up-stroke* mode (transfer ratio: 1.0) display the attraction which extends in pure water to only ca. 30 nm, although their pull-off forces are the same as those for the down-stroke preparations (200–300 mN/m, which corresponds to the interfacial energy of 21–32 mJ/m^2). Therefore, the long-range attraction is very sensitive to small structural differences of the hydrophobic surface. The unprecedented long-range attraction cannot be readily accommodated previous explanations which are based on conventional hydration force and cavitation. The concept of "vicinal water" by Drost-Hansen can be an alternative basis of the observed attraction. We propose that the structural correlation of interfacial water extend to the submicron range, if the interface is sufficiently large, molecularly smooth, and strongly hydrophobic. The enhanced structural correlation leads to long-range attraction.

Introduction

"The hydrophobic effect" is commonly used to express specific properties of nonpolar molecules in water. The "hydrophobic" attraction between nonpolar (hydrophobic) molecules and surfaces in water cannot be fully accounted for by continuum theories of van der Waals forces.[1-3] Interactions between macroscopic hydrophobic surfaces are treated as an extension of these molecular effects. However, recent reports suggest that interactions between nonpolar surfaces in water are more complicated than have been thought. In particular, Drost-Hansen postulated formation of ordered water structures at solid interfaces along with possible existence of long-range order.[4-6] The water molecules on hydrophobic surfaces were considered to become structured in clathrate-like ordering which extends to tens and hundreds (or more) of molecular diameters, while those on polar surfaces were considered to be oriented by dipole–dipole interaction. This effect was thought to affect properties of water near surfaces and physicochemical properties of dispersed systems.

The forces between surfaces can be directly measured by a surface forces apparatus. The force–distance profile is related to the mode of surface interactions. The attractive force, which is much stronger than the conventional van der Waals force and counteracts the electrostatic repulsion, was first reported between hydrophobic adsorbed layers of trimethylcetylammonium bromide on mica.[7] Although the net interaction was repulsive, the estimated attractive component at distances of several nanometers was two orders of magnitude larger than expected from the van der Waals force, and decreased exponentially with a decay length of 1 nm. More recently, *net* attraction extending to even longer distances was reported.[8,9] In these measurements, surfaces were considered to be more hydrophobic than previous preparations, and the distance where observable attraction appears varied depending on sample preparations. More recently, uncharged hydrocarbon and fluorocarbon surfaces (no observable repulsion) prepared by the Langmuir–Blodgett (LB) technique produced attraction extending to a separation of 80 nm in pure water.[10,11] An exponential function with two decay lengths of 2–3 and 13–16 nm was found to fit the experimental data. The origin of the long-range attraction is not yet fully understood, although several

* To whom correspondence should be addressed.
[‡] Present address: Department of Applied Physics and Department of Quantum Engineering, School of Engineering, Nagoya University, Chikusa, Nagoya 464-01, Japan.
[†] Permanent Address: Faculty of Engineering, Kyushu University, Fukuoka 812, Japan.

(1) Israelachvili, J. N. *Intermolecular and Surface Forces*: Academic Press: London, 1985.
(2) Muller, N. *Acc. Chem. Res.* **1990**, *23*, 23–28.
(3) Tanford, C. *The Hydrophobic Effect*; John Wiley: New York, 1980.
(4) Etzler, F. M.; Conners, J. J. *Langmuir* **1990**, *6*, 1250–1253.
(5) Drost-Hansen, W. *Ind. Eng. Chem.* **1969**, *61*, 10–47.
(6) Etzler, F. M.; Drost-Hansen, W. *Croat. Chem. Acta* **1983**, *56*, 563–592.
(7) Israelachvili, J. N.; Pashley, R. M. *J. Colloid Interface Sci.* **1984**, *98*, 500–514.
(8) Pashley, R. M.; McGuiggan, P. M.; Ninham, B. W.; Evans, D. F. *Science* **1985**, *229*, 1088–1089.
(9) Claesson, P. M.; Blom, C. E.; Herder, P. C.; Ninham, B. W. *J. Colloid Interface Sci.* **1986**, *114*, 234–242.
(10) Claesson, P. M.; Christenson, H. K. *J. Phys. Chem.* **1988**, *92*, 1650–1655.
(11) Christenson, H. K.; Claesson, P. M.; Berg, J.; Herder, P. C. *J. Phys. Chem.* **1989**, *93*, 1472–1478.

0002-7863/92/1514-10927$03.00/0